Supporting Information

Ellingsen et al. 10.1073/pnas.1305050110

SI Results

Behavioral Results. ***Relationship between initial expectations and placebo responses.*** Expectation of treatment benefit is often an important factor in shaping placebo responses. We therefore calculated correlation coefficients between the agreement with questionnaire statements suggesting nasal spray benefit, and the placebo-induced change in visual analog scale (VAS) hedonic ratings, within each stimulus type (Fig. S1). Expectation of increased warm pleasantness significantly correlated with placebo warm hyperhedonia ($r = 0.33$; $P = 0.04$, one-tailed), and expectation of reduced pain unpleasantness significantly correlated with placebo analgesia ($r = 0.55$; $P = 0.001$, one-tailed). The correlation between expectation of increased stroking touch pleasantness and placebo stroking hyperhedonia was also positive, but did not reach statistical significance ($r = 0.1$; $P = 0.32$, one-tailed).

Effects of order and sex. As confirmed by repeated-measures ANOVAs, there were no significant effects of treatment order or sex on expectation ratings (all P's > 0.5) or hedonic ratings (all P's > 0.42).

Temporal characteristics of hedonic ratings. To investigate whether VAS reports stayed consistent throughout the experimental sessions, we first calculated mean values from the first and the last half of the experimental sessions for each individual. We then performed a repeated-measures ANOVA with the factors stimulus type (stroking, warm, pain), and time (first half, last half). There was no significant main effect of time [$F(1, 27) = 2.1$, $P = 0.16$] and no significant interaction between time and stimulus type [$F(1.3, 36) = 0.85$, $P = 0.4$]. In post hoc t tests (paired, two-tailed) comparing the first and last halves within each stimulus type, we found no significant differences of time for the ratings of stroking ($P = 0.29$) and painful touch ($P = 0.85$). However, the ratings of warm touch were significantly higher in the first half compared with the last half of the experimental sessions ($P = 0.02$), which may be related to the decrease in temperature (the HotCold pack decreased slightly in temperature from ∼42.5 °C at the start, to ∼40 °C at the end), satiety of the stimulus, or other effects of lying in an MRI scanner for this period. The effects did not significantly differ between placebo and control sessions (all $P = 0.2$). Nor did the decline in warm ratings differ significantly from decline in stroking touch ($P = 0.3$) or pain ratings ($P = 0.1$).

Functional MRI Results. ***Relationship between initial expectations and placebo-induced blood-oxygen level-dependent change.*** To explore the relationship between initial expectation and placebo-induced (placebo-control) blood-oxygen level-dependent (BOLD) changes, we added a regressor with the expectation of treatment benefit (demeaned) for each stimulus type for the functional MRI (fMRI) analysis setup (placebo > control) for each stimulus, controlling for multiple comparisons within regions of interest (ROIs) encompassing emotion appraisal and sensory circuitry (Fig. S6). There was a correlation between expectation of treatment benefit on stroking touch and placebo-induced increase in the posterior insula (pINS) during stroking touch ($Z = 2.45$, contralateral to the stimulus site), but nothing else survived significance threshold. However, an activation pattern generally comparable (but weaker) to analyses using placebo response as a regressor, was observed when thresholding at $P = 0.05$ (uncorrected) (Fig. S3).

Outlier correction. Two subjects in the comparison between [placebo-induced medial orbitofrontal cortex (mOFC)–periaqueductal gray (PAG) coupling] and [placebo-induced BOLD change in the secondary somatosensory area (SII)] during pain (Fig. 4), are outside of ±1.5-times the interquartile range: −0.94 to 1.1; they can be considered mild outliers according to the guidelines of ref. 1. If these subjects are both excluded from analysis, the effect remains comparable to the original analysis ($r_{stroking} = 0.31$, $r_{pain} = -0.21$; $Z = 1.9$, $P = 0.03$). Furthermore, the results remain the same when conducting the voxel-based analysis using robust outlier deweighting (as implemented in FLAME [Functional MRI of the Brain's (FMRIB) Local Analysis of Mixed Effects], FSL) ($Z = 2.85$).

SI Materials and Methods

Balance of the Conditions. The placebo and control conditions were carried out on separate days to keep the sessions as short as possible, to maximize participants' comfort. To ensure experimental balance, the two sessions were kept as identical as possible, both before and during the experimental procedure. Before both experimental sessions, the participants went through the exact same sequence of temperatures during pain thresholding, watched the video documentary, and filled out the expectation and mood questionnaires. During both experiments the participants received the same tactile stimuli, which were administered by an experimenter who was blinded to which session it was (placebo or control). The only aspect that differed was the nasal spray administration, which was done in the placebo session only. Although there was no sensory stimulation of the nostrils in the control session, we consider it an unlikely cause of the hyperhedonic and analgesic effects that were observed in the experiment, which started ∼10 min after nasal spray administration.

Video Documentary About Oxytocin. To induce expectation of intranasal oxytocin's beneficial effects on painful and pleasant touch experience, participants viewed a 6-min locally developed video documentary about oxytocin's putative prosocial effects such as involvement in bonding, love, grooming, affective touch, and healing. As all of the material was based on published research, there was no deception. The video concluded that a nasal spray of oxytocin might enhance the pleasantness of: (*i*) stroking and (*ii*) warm touch, and (*iii*) reduce the unpleasantness of pain. The video was introduced using a scripted explanation: "Due to the recent surge in scientific and media interest in oxytocin's positive effects in humans, how much people know about oxytocin varies greatly. Thus, we show everyone this film to even out the differences." Participants viewed the video in both sessions.

Mood Assessment. Mood was measured at three time points during each session: (*i*) after informed consent, (*ii*) immediately before scanning, and (*iii*) immediately after scanning. Participants rated their current level of fear, sadness, irritability, happiness, calmness, and anxiety using VAS with anchors "not at all" and "very much so." These scores were analyzed using repeated-measures ANOVA with the within-subjects factors treatment (placebo, control), time of rating (*i*, *ii*, *iii*), and questionnaire item, and between-subjects factors treatment order (placebo first, control first) and sex (male, female). There were no significant main effects or interactions (all Fs < 2.23; all Ps > 0.06).

Assessment of Expectations. After watching the video documentary about oxytocin, participants filled in a questionnaire (−3 to +3 Likert scale, with the anchors "completely disagree" and "completely agree") addressing specific expectations about effects of intranasal oxytocin. This questionnaire included 10 items, all starting with "I believe a nasal spray containing oxytocin will make me…" and ending either with relevant statements (experience

touch as more pleasant, warmth as more pleasant, pain as less unpleasant) or with control items (feel more outgoing and social, feel less patient, discriminate better between moving touch velocities, feel touch as unpleasant, feel happier, more relaxed, feel generally more delighted). Participants filled in the same questionnaire in both sessions. Expectation data were analyzed used repeated-measures ANOVA (Greenhouse–Geisser correction) with the within-subjects factors session number (session 1, session 2) and questionnaire item (each of the 10 items), and the between-subjects factors treatment order (placebo first, control first) and sex (male, female). The reports did not differ between the two sessions [$F(1,20) = 1.2$, $P = 0.3$]. We performed direct comparisons between relevant and irrelevant statements using averaged values from both sessions. Planned paired t tests (one-tailed) between the response on each relevant item (expectation of increased stroking and warm touch pleasantness, and reduced unpleasantness of pain) and the averaged responses on the irrelevant items, were calculated.

MRI Acquisition and Preprocessing. Imaging was performed using a Philips Achieva 3 Tesla whole-body MR unit equipped with an eight-channel Philips SENSE (reduction factor = 2) head coil (Philips Medical Systems). Functional images were acquired with a gradient-echo echo-planar imaging (EPI) sequence: TR = 2000 ms; TE = 30 ms; flip angle = 80°; field-of-view = 240 × 240; in-plane resolution = 3 × 3 mm; slice thickness = 3 mm; gap spacing between slices = 0.3 mm; number of axial slices (placed on the ac-pc line) = 34; number of volumes = 510. A high-resolution T1-weighted scan was acquired directly after the fMRI sequence in session two, to aid registration of the EPI images to standard space: TR = 7.1 ms; TE = 3.2 ms; flip angle = 8°; field-of-view = 256 × 256; in-plane resolution = 1 × 1 mm; slice thickness = 1 mm (no gap); number of axial slices = 160.

Prestatistics processing was applied within each individual run: motion correction using MCFLIRT (2); nonbrain removal using BET (3); spatial smoothing using a Gaussian kernel of full-width half-maxim 5 mm; grand-mean intensity normalization of the entire 4D dataset by a single multiplicative factor; high pass temporal filtering (Gaussian-weighted least-squares straight line fitting with a high pass filter cutoff of 120.0 s).

We applied a denoising procedure using probabilistic independent component analysis (ICA) (4) as implemented in MELODIC (Multivariate Exploratory Linear Decomposition into Independent Components) v3.10. Independent components were visually inspected, and labeled noise-components or signal-components, following the guidelines presented by Kelly, et al. (5). The time courses of noise-components were filtered out from the preprocessed data, and the resulting denoised data were used in the statistical analyses. An example of the effect of denoising on pain signal in the PAG/colliculi is illustrated in Fig. S4 and Table S3.

Registration of small structures in the brainstem to a standard template is not straight-forward. We therefore compared the registration procedure (FLIRT) used in this study with an alternative procedure (FLIRT plus FMRIB's nonlinear registration technique, FNIRT). The two procedures provided comparable registration quality and statistical effects.

fMRI Analysis. ***Regions of interest.*** All a priori ROIs were defined from independent sources. ROIs in contralateral parts of the sensory circuitry comprised: (*i*) posterior insula (pINS/Ig2, $P > 30\%$); (*ii*) primary somatosensory area (SI/area 3b, $P > 50\%$); (*iii*) secondary somatosensory area (SII/OP4, $P > 50\%$): Jülich histological atlas (6); and (*iv*) sensory thalamus Oxford thalamic connectivity probability atlas ($P > 10\%$) (7). Very few voxels are more than 50% probable of being in the pINS/Ig2 and the sensory thalamus in the Montreal Neurological Institute (MNI)152 standard map. Therefore, to ensure enough space was provided for detecting effects within these structures, thresholds for these ROIs were lowered to 30% and 10%, respectively, thereby reducing the risk of type II errors (see Fig. S6 for illustrations of all ROIs overlaid on a MNI152 standard brain).

ROIs defined within emotion appraisal circuitry comprised: (*i*) the pregenual anterior cingulate cortex (pgACC) and (*ii*) mOFC [spheres (8-mm radius) around peak activations from a meta-analysis of placebo analgesia (8)]; (*iii*) the nucleus accumbens (NAc) and (*iv*) amygdala (Harvard-Oxford subcortical atlas, $P > 50\%$); (v) the PAG (mask used by ref. 9); and (*vi*) the ventral tegmental area [VTA; manually drawn based on anatomical landmarks from the Duvernoy's Brainstem atlas (10), ranging from MNI152 coordinates z (−10) to z (−18)]. Selection of the regions (mOFC, pgACC, PAG) for the comparison between placebo-induced ventromedial prefrontal cortex (vmPFC)–PAG functional coupling and placebo-induced change in sensory regions was based on a priori predictions derived from this circuit's involvement in placebo analgesia (9, 11, 12). This selection was made irrespective of these regions' activation in the basic contrast (placebo > control) because of the individual variability in placebo response magnitude.

To investigate whether structures outside the hypothesized circuitry were important for placebo hyperhedonia or analgesia, we performed voxel-based analyses using a whole-brain approach with a corrected cluster significance threshold of $P = 0.05$ (13). Because we did not observe any additional activations that furthered our understanding of the current findings, these results are presented in Table S4 without further discussion.

Conjunction analysis. To formally test whether any voxels were significantly activated (placebo > control) during both stroking, warm, and painful touch, we calculated a minimum Z image to test the "conjunction null" hypothesis (14).

1. Tukey JW (1977) *Exploratory Data Analysis* (Addison-Wesly, Reading, MA).
2. Jenkinson M, Bannister P, Brady M, Smith S (2002) Improved optimization for the robust and accurate linear registration and motion correction of brain images. *Neuroimage* 17(2):825–841.
3. Smith SM (2002) Fast robust automated brain extraction. *Hum Brain Mapp* 17(3):143–155.
4. Beckmann CF, Smith SM (2004) Probabilistic independent component analysis for functional magnetic resonance imaging. *IEEE Trans Med Imaging* 23(2):137–152.
5. Kelly RE, Jr., et al. (2010) Visual inspection of independent components: Defining a procedure for artifact removal from fMRI data. *J Neurosci Methods* 189(2):233–245.
6. Eickhoff SB, et al. (2007) Assignment of functional activations to probabilistic cytoarchitectonic areas revisited. *Neuroimage* 36(3):511–521.
7. Behrens TE, et al. (2003) Non-invasive mapping of connections between human thalamus and cortex using diffusion imaging. *Nat Neurosci* 6(7):750–757.
8. Amanzio M, Benedetti F, Porro CA, Palermo S, Cauda F (2013) Activation likelihood estimation meta-analysis of brain correlates of placebo analgesia in human experimental pain. *Hum Brain Mapp* 34(3):738–752.
9. Eippert F, et al. (2009) Activation of the opioidergic descending pain control system underlies placebo analgesia. *Neuron* 63(4):533–543.
10. Naidich TP, et al. (2009) *Duvernoy's Atlas of the Human Brain Stem and Cerebellum* (Springer, New York, NY).
11. Bingel U, Lorenz J, Schoell E, Weiller C, Büchel C (2006) Mechanisms of placebo analgesia: rACC recruitment of a subcortical antinociceptive network. *Pain* 120(1–2):8–15.
12. Wager TD, Scott DJ, Zubieta JK (2007) Placebo effects on human mu-opioid activity during pain. *Proc Natl Acad Sci USA* 104(26):11056–11061.
13. Worsley KJ (2001) Statistical analysis of activation images. *Functional MRI: An Introduction to Methods*, eds Jezzard P, Matthews PM, Smith SM (OUP, Oxford).
14. Nichols T, Brett M, Andersson J, Wager T, Poline JB (2005) Valid conjunction inference with the minimum statistic. *Neuroimage* 25(3):653–660.

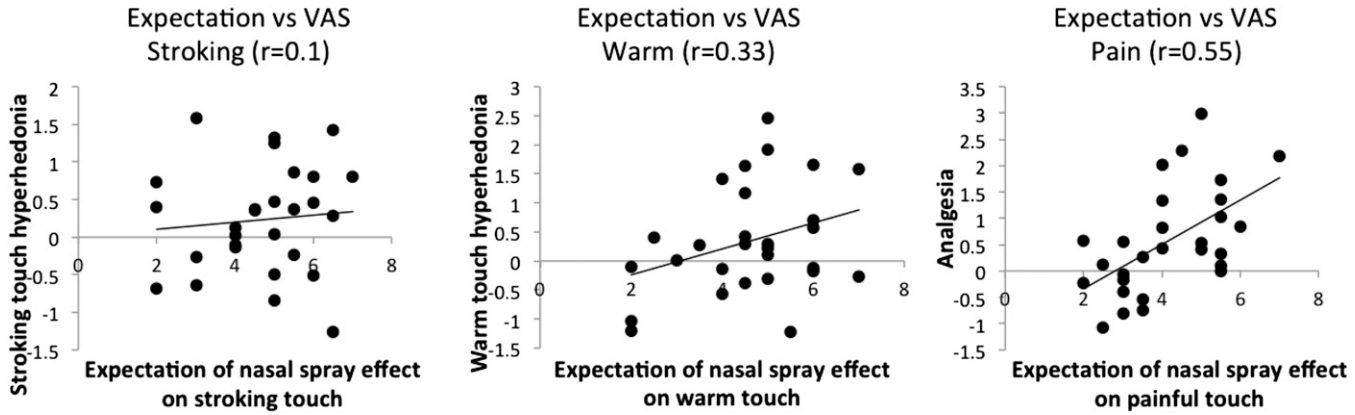

Fig. S1. Relationship between expectations and placebo responses. Expectations of nasal spray benefit on tactile stimuli had a positive relationship with placebo response (defined as the placebo minus control difference in VAS scores) for stroking (nonsignificant), warm, and painful touch.

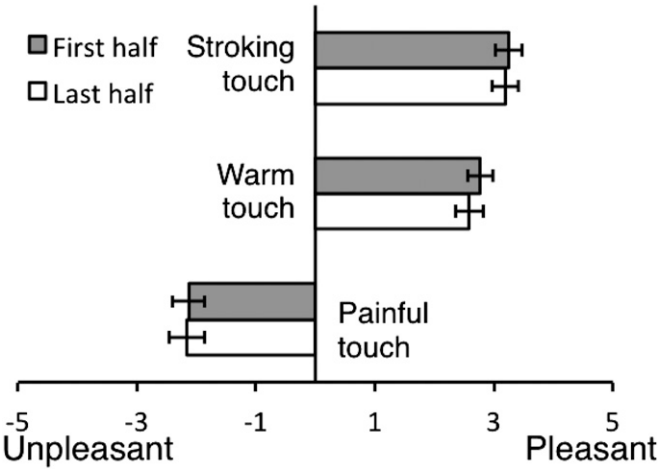

Fig. S2. Temporal characteristics of hedonic ratings. There was no main effect of time (first half vs. last half of the experiment) on ratings. Post hoc *t* tests indicated that although ratings of stroking and painful touch did not differ significantly over time, ratings of warm touch were significantly higher in the first half. However, the decline in warm touch ratings did not differ significantly between placebo and control sessions, nor did it differ significantly from decline in stroking or painful touch. Error bars indicate SEM.

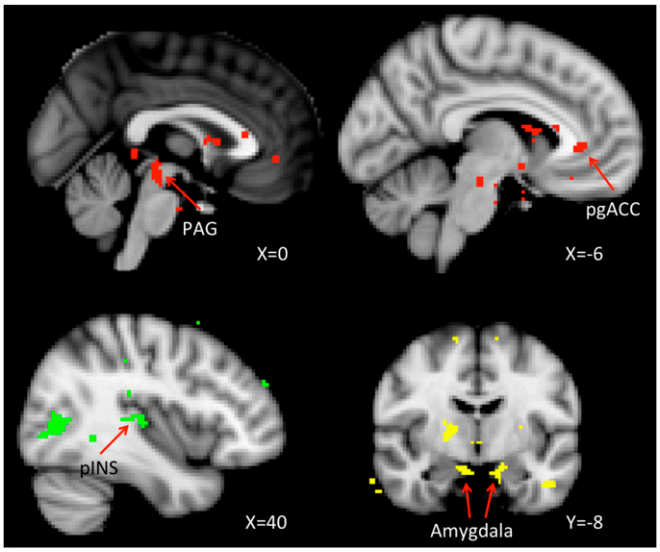

Fig. S3. Exploratory analyses using expectation of nasal spray benefit as a regressor. Averaged group activation maps ($P > 0.05$ uncorrected, whole-brain), with the expectation of nasal spray benefit as a regressor, are superimposed on the MNI standard template brain. Green, stroking touch; yellow, warm touch; red, painful touch.

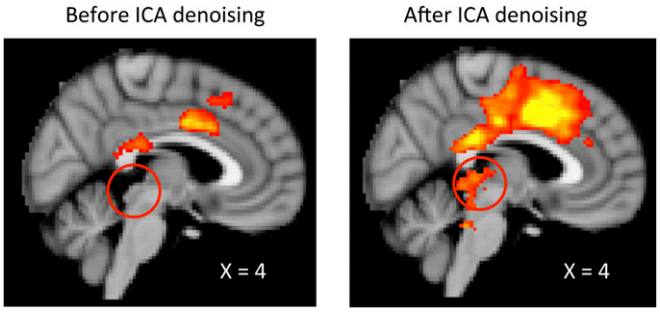

Fig. S4. Effect of ICA denoising on baseline pain signal. Stimulus signal increased substantially after denoising using ICA, here illustrated by increased signal in PAG/colliculi. Significant voxels from the group contrast pain > rest, in the control session, are shown (whole-brain search, cluster-thresholded at $Z = 2.3$).

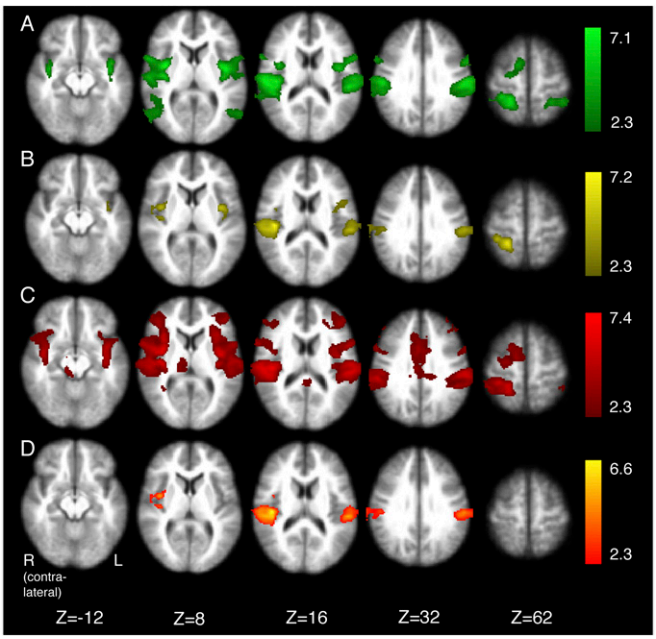

Fig. S5. Baseline stimulus activation maps. BOLD responses (stimulus > rest, control condition) during stroking touch (*A*), warm touch (*B*), and painful touch (*C*), and voxels overlapping between all three touch stimuli, as revealed by conjunction analysis (*D*). Color bars to the right indicate *Z*-scores (ranging from minimum value to maximum value in the contrast), and MNI-coordinates are shown in millimeters. Averaged group activation maps (cluster-thresholded, whole-brain) are superimposed on the MNI-registered (group average) structural image (T1-weighted).

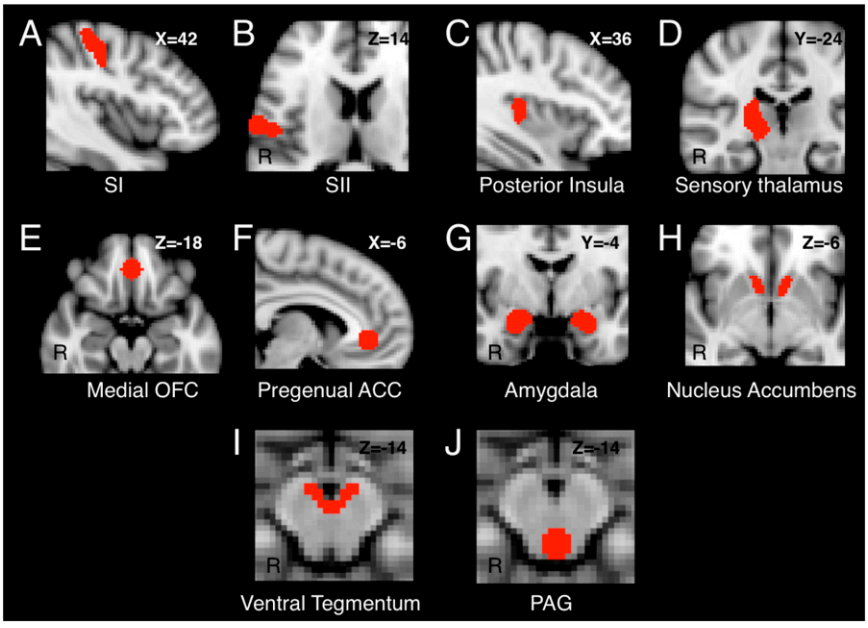

Fig. S6. A priori regions of interest. Masks used for analyses assessing sensory circuitry were right primary somatosensory area (*A*), right secondary somatosensory area (*B*), right pINS (*C*), and right sensory thalamus (*D*), all contralateral to the stimulus site. Masks used for analyses assessing emotion appraisal circuitry were medial orbitofrontal cortex (*E*), pregenual anterior cingulate (*F*), amygdala (*G*), nucleus accumbens (*H*), ventral tegmentum (*I*), and periaqueductal gray (*J*). Masks are superimposed on the MNI standard template brain, and MNI coordinates are shown in millimeters.

Table S1. BOLD responses in sensory circuitry

Analysis	pINS	SI	SII	Sensory thalamus
Group contrast ($P > C$)				
Stroking	3.96 (40 −20 10)	—	3.25 (54 −12 12)	—
Warm	3.26 (40 −20 6)	—	2.33 (68 −14 18)	—
Painful	—	−4.29 (20 −34 60)	−3.56 (56 −4 12)	—
Pleasant touch ($P > C$) > Painful touch ($P > C$)				
Stroking ($P > C$) > Pain ($P > C$)	2.27 (40 −22 16)	3.13 (42 −24 60)	3.39 (52 −12 18)	—
Warm ($P > C$) > Pain ($P > C$)	2.27 (36 −22 4)	3.44 (46 −20 50)	2.57 (60 −4 12)	—
Correlation with behavioral placebo response				
Stroking	3.1 (34 −24 12)	3.11 (20 −34 66)	—	—
Warm	—	—	—	—
Painful	—	—	—	—
Correlation with placebo-induced vmPFC-PAG coupling				
Stroking	mOFC-PAG: 2.37 (34 −20 6)	—	mOFC-PAG: 3.01 (56 −6 14) pgACC-PAG: 2.79 (54 −8 10)	—
Warm	—	—	pgACC-PAG: 2.38 (52 −12 16)	—
Painful	mOFC-PAG: 2.51 (36 −24 18)	pgACC-PAG: 4.77 (56 −4 24)	mOFC-PAG: 2.85 (60 −10 10)	—

The strength of activation is expressed in maximum (peak) *Z* scores, and coordinates in MNI-space are denoted by *x*, *y*, *z* in millimeters [*Z* (*x y z*)]. The listed *Z* scores survived significance threshold ($P = 0.05$, corrected for small volumes). C, control; L, left; mOFC, medial orbitofrontal cortex; P, placebo; PAG, periaqueductal gray; pgACC, pregenual anterior cingulate cortex; R, right; SI, primary somatosensory area; SII, secondary somatosensory area.

Table S2. BOLD responses in emotion appraisal circuitry

Analysis	pgACC	mOFC	NAc	Amygdala	PAG	VTA
Group contrast ($P > C$)						
Stroking	—	—	2.92 (12 18 −4)	—	3.16 (−6 −32 −2)	—
Warm	—	—	4.69 (12 18 −6)	2.06 (−16 −2 −19)	2.59 (−4 −30 −6)	2.31 (−6 −14 −16)
Painful	—	—	3.51 (14 18 −4)	—	—	2.29 (−8 −14 −16)
Correlation with behavioral placebo response						
Stroking	3.7 (−6 10 −4)	2.8 (4 46 −20)	3.2 (−10 10 −12)	—	4.1 (−2 −30 −8)	3.8 (4 −16 −14)
Warm	—	—	2.98 (−6 10 −4)	2.9 (−16 −8 −18)	—	2.75 (−2 −20 −16)
Painful	3.18 (−6 36 2)	—	—	—	—	—
PPI Group contrast ($P > C$)						
Stroking (mOFC seed)	—	—	—	—	2.4 (2 −30 −14)	—
Warm	—	—	—	—	—	—
Painful (pgACC seed)	—	—	—	—	3.3 (−2 −30 −8)	—
PPI correlation with placebo response						
Stroking (mOFC seed)	—	—	2.35 (−12 14 −6)	2.94 (−22 −8 −14)	2.98 (4 −30 −6)	—
Warm	—	—	—	—	—	—
Painful (pgACC seed)	—	3.18 (8 44 −18)	3.46 (12 10 −10)	2.84 (−26 −2 −16) (L) 3.24 (18 −6 −18) (R)	—	3.04 (4 −20 −20)

The strength of activation is expressed in maximum (peak) *Z* scores, and coordinates in MNI-space are denoted by *x*, *y*, *z* in millimeters [*Z* (*x y z*)]. The listed *Z* scores survived significance threshold ($P = 0.05$, corrected for small volumes). pgACC, pregenual anterior cingulate cortex; mOFC, medial orbitofrontal cortex; NAc, nucleus accumbens; PAG, periaqueductal gray; VTA, ventral tegmental area; PPI, psychophysiological interaction analysis; P, placebo; C, control; R, right; L, left.

Table S3. Comparison between *Z*-scores before and after ICA denoising

Contrast	Peak *Z* (PAG ROI)	
	Before ICA	After ICA
Pain > Rest (Control session)	1.46	3.33
Group contrast (Placebo > Control)	0.49	0.94

PAG, periaqueductal gray; ROI, region of interest; ICA, independent component analysis.

Table S4. BOLD responses (whole-brain searches)

Analysis	*Z* (*x y z*)
Group contrast (*P* > C)	
Stroking touch	
Superior temporal gyrus	3.74 (−70 −24 10)
Correlation (*P* > C)	
Stroking touch	
Subcallosal cortex	4.00 (−6 22 −8)
Cuneal cortex	3.78 (−20 −72 24)
Precuneous	3.86 (−6 −50 46)
Painful touch	
Superior temporal gyrus	4.21 (−56 −36 12)
PPI mOFC (*P* > C)	
Stroking touch	
Anterior cingulate cortex	3.45 (−10 10 38)
PPI pgACC (*P* > C)	
Warm touch	
Precuneous	3.38 (8 −56 34)
Painful touch	
Frontal pole	3.72 (2 70 −18)
Occipital cortex	3.43 (-4 −98 24)

The strength of activation is expressed in maximum (peak) *Z* scores, and coordinates in MNI-space are denoted by *x*, *y*, *z* in millimeters [*Z* (*x y z*)]. The listed *Z* scores survived significance threshold (*P* = 0.05, whole-brain cluster corrected). P, placebo; C, control; PPI, psychophysiological interaction analysis; mOFC, medial orbitofrontal cortex; pgACC, pregenual anterior cingulate cortex.